

Comparative Analysis of Dynamic Electrochemical Test Methods of Supercapacitors

Z. Stevic^{1,*}, M. Rajcic-Vujasinovic¹ and I. Radovanovic²

¹ University of Belgrade, Technical faculty, Bor, Serbia

² Innovation center of School of Electrical Engineering, University of Belgrade, Belgrade, Serbia

*E-mail: zstevic@tf.bor.ac.rs ; zstevic@live.com

Received: 9 September 2013 / *Accepted:* 26 June 2014 / *Published:* 29 September 2014

Supercapacitor investigation due to the high capacitance, therefore long time constants, requires considerable modification and adaptation of classical electrochemical methods and instrumental techniques. This paper presents a mathematical analysis, which defines the parameters of the experimental methods, modified standard methods (galvanostatic, potentiostatic, ALSV), as well as new one - tilting current excitation. Firstly, the methods are tested on a specially constructed physical model - the electrical circuit with commercial super capacitor of 1.6 F, as well as the computer simulation. The measurements were performed on a specially developed measuring system based on PC and LabVIEW package. All the methods are applied in the development of a new type of supercapacitor based on natural copper minerals - chalcocite (Cu₂S). Comparative methods analysis in terms of efficiency and accuracy is given in the paper.

Keywords: Supercapacitors, Electrochemical methods, Mathematical Model, LabVIEW, Equivalent electrical circuit

1. INTRODUCTION

There are a number of standard methods for the examination of electrochemical systems that are used for supercapacitor testing [1-8]. In this paper, most important standard methods are presented along with their modification proposals, and also some more suitable methods for testing various supercapacitor parameters are presented.

In order to monitor the process on only one electrode (electrode-electrolyte interface) the application of three-electrode electrochemical cell [9] is common. The cell is powered by working (WE) and counter electrode (CE), and the working electrode potential is measured against a reference (RE) one. As the reference electrode in this approach, it is commonly used calomel electrode. The working electrode is made of a material whose behavior in a particular electrolyte is being examined,

and counter electrode is made of platinum or other conductive material which is insoluble in that particular electrolyte.

Depending on the wanted accuracy, possible duration of the test or equipment availability, different electrochemical system testing methods are applied. Comparative analysis of the most suitable dynamic methods for supercapacitor testing is presented in this paper.

2. PROCESS MODELING DUE TO DIFFERENT EXCITATIONS

Different signal excitations are defining particular testing methods for electrochemical systems. For this analysis, the following methods have been chosen: galvanostatic, potentiostatic, swiping voltage and current and cyclic voltammetry. For every particular method, mathematical model is derived and system response is defined for given excitation. Also, the algorithms for system parameters extraction are given, based on experimentally obtained response diagrams.

2.1. Galvanostatic Method

In galvanostatic electrochemical method, excitation of a system is pulse current of constant intensity (I) and the settable duration [1,10-12].

Response, the voltage between the working electrode (WE) and the reference electrode (RE) is being monitored on an electronic millivoltmeter and plotter (EMVP) or, more recently through AD converters on the computer [13]. It is important that the input resistance EMVP has to be very high (order of $10^{12} \Omega$ or more) because of the reference electrode tremendous internal resistance. In electrochemistry this specified voltage is often called overvoltage [1] (referring to the additional voltage between WE and RE given in regard to the voltage between these electrodes when there is no excitation current).

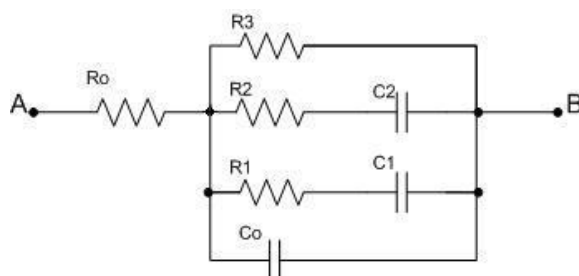


Figure 1. Equivalent circuit for the observed class of electrochemical systems

Standard galvanostatic method in the processing of the experimental data is based on a very simplified model of electrochemical system (in series RC circuit) and cannot be used in the case of supercapacitor. Therefore, it was necessary to modify this method and refine the model and the procedure for obtaining the model parameters [11]. The equivalent electrical circuit is determined,

which response to the galvanostatic pulse is practically the same as for the observed electrochemical system (Fig. 1.) [10, 11, 14-24].

Resistance R_0 physically corresponds to the resistance of the electrolyte and the electrode material together, and its value is in the order of ohms. Capacitance C_0 (order of magnitude μF) corresponds to the dual layer that is formed on the side of the electrolyte. Resistance R_1 and R_2 (the order of magnitude of tens of ohms) are related to the slow processes of adsorption and diffusion, as well as the capacitor C_1 (mF) and C_2 (F). R_3 is the resistance of self-discharge, so it is reciprocally connected with electricity leakage. Its value is in the order of hundreds of ohms to several kilohms.

Taking into account the magnitudes of capacitance C_0 , C_1 and C_2 , the secondary region of galvanostatic pulses, it is possible to simplified the equivalent circuit by omitting the capacitor C_0 , which is not an essential when it comes to supercapacitors (Fig. 2.).

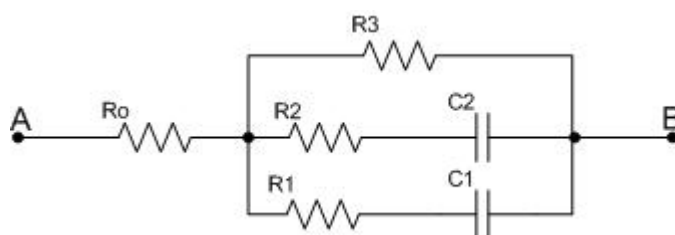


Figure 2. Simplified equivalent circuit

Complex images of overvoltage η , ie voltage U_{AB} is:

$$\eta (S) = U_{AB}(S) = I(S) \cdot Z_{AB}(S) = \frac{I}{S} Z_{AB}(S)$$

$$\eta (S) = R_0 I / S + I \frac{S^2 R_1 R_2 R_3 C_1 C_2 + S(R_1 R_3 C_1 + R_2 R_3 C_2) + R_3}{S(S^2((R_1 + R_2)C_1 C_2 R_3 + R_1 R_2 C_1 C_2) + S((C_1 + C_2)R_3 + R_1 C_1 + R_2 C_2) + 1)}$$

The resulting expression is quite complex, but it can be significantly simplified assuming that $C_2 \gg C_1$, which is physically realistic. By applying the Heaviside expansion formula overvoltage is obtained in the time domain:

$$\eta(t) = (R_0 + R_{23})I \left(1 - e^{-\frac{t}{\tau_1}}\right) + \frac{R_3^2}{R_2 + R_3} I \left(1 - e^{-\frac{t}{\tau_2}}\right)$$

or in a slightly different form:

$$\eta(t) = (R_0 + R_{23})I \left(1 - e^{-\frac{t}{\tau_1}}\right) + (R_3 - R_{23})I \left(1 - e^{-\frac{t}{\tau_2}}\right)$$

whereby:

$$R_{23} = \frac{R_2 R_3}{R_2 + R_3} \quad (\text{parallel connection } R_2 \text{ and } R_3)$$

$$\tau_1 = (R_1 + R_{23})C_1 \text{ (time constant of the first phase)}$$

$$\tau_2 = (R_2 + R_3)C_2 \text{ (time constant of the second phase)}$$

Typical appearance of galvanostatic curve with characteristic data from which it is possible to calculate all parameters of equivalent circuit is shown in Fig 3.

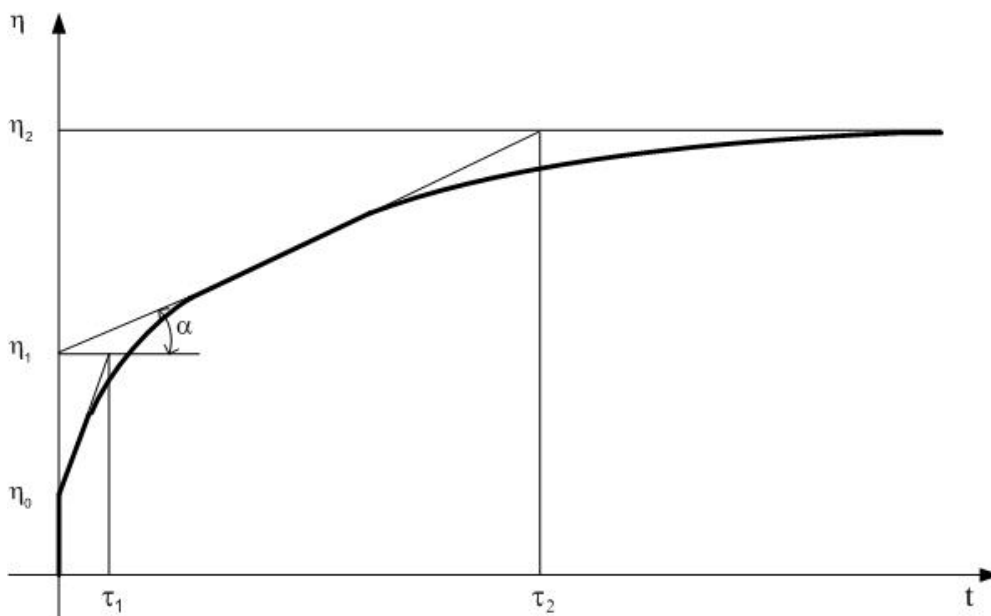


Figure 3. Typical galvanostatic curve of observed electrochemical systems

If a complete galvanostatic curve is recorded (during the pulse duration greater than $4 \tau_2$ to achieve a stationary level η_2 , which is quite a long time - the order of thousands of seconds), the procedure for obtaining the parameters of the circuit would be as the following:

1. Evaluation of the value of R_0 compared to the other resistance. If R_0 cannot be ignored it is necessary to make additional galvanostatic experiment with the same intensity of current, but with the time duration in order of μs . Then the intercept η on the axis is:

$$\eta_{00} = R_0 I \text{ (} C_0 \text{ is short-circuit in such a short time)}$$

which implies:

$$R_0 = \frac{\eta_{00}}{I}$$

2. From the diagram (Fig 3.) it is obvious that:

$$\eta_2 = (R_0 + R_3) I$$

$$\text{therefore: } R_3 = \frac{\eta_2}{I} - R_0$$

3. From the diagram (Fig 3.): $\eta_1 = (R_0 + R_{23}) I$

therefore: $R_2 = \frac{R_3(\eta_1 - R_0 I)}{(R_0 + R_3)I - \eta_1}$

4. From the diagram (Fig 3.):

$\eta_0 = (R_0 + R_{123}) I$ (R_{123} parallel connection R_1, R_2, R_3)

therefore:

$R_1 = \frac{(\eta_0 - R_0 I)R_{23}}{(R_0 + R_{23})I - \eta_0}$

5. From the diagram (Fig 3.) time constant τ_1 is:

$\tau_1 = (R_1 + R_{23}) C_1$

therefore, the capacitance can be calculated:

$C_1 = \frac{\tau_1}{R_1 + R_{23}}$

6. From the diagram (Fig 3.) time constant τ_2 is:

$\tau_2 = (R_2 + R_3) C_2$

therefore, C_2 can be calculated:

$C_2 = \frac{\tau_2}{R_2 + R_3}$

It should be noted that the C_2 , as the most important parameter of the circuit when it comes to supercapacitors, can be determined from a short pulse of galvanostatic, from the slope of the linear part of the galvanostatic curve. The only problem is that firstly it is necessary to determine the resistance R_3 (potentiostatic method or some other method). For determined R_3 and calculated R_2 following the instructions given in the point 3. of this method, C_2 can be determined from:

$tg \alpha = \frac{R_3^2}{(R_2 + R_3)^2} \frac{I}{C_2} \Rightarrow C_2 = \frac{R_3^2 I}{(R_2 + R_3)^2 tg \alpha}$

Where, $tg \alpha$ (Fig 3) is the slope of the linear part of the galvanostatic curve, ie. the numerical value of derivative $\frac{d\eta}{dt}$ in that area, expressed in V / s.

2.2. Potentiostatic Method

In this method, the excitation is a constant impulse overvoltage E, and the response is monitored as current change in time, therefore, this method is often referred to as chronoamperometry [1].

Voltage and its complex image is:

$\eta(t) = E \cdot h(t), \quad \eta(S) = \frac{E}{S},$

therefore, the current for the equivalent circuit:

$$i(S) = \eta(S) \cdot \frac{1}{Z(S)} = \frac{E}{S} \frac{1}{R_0 + \frac{S^2 R_1 R_2 R_3 C_1 C_2 + S(R_1 R_3 C_1 + R_2 R_3 C_2) + R_3}{S^2((R_1 + R_2)C_1 C_2 R_3 + R_1 R_2 C_1 C_2) + S((C_1 + C_2)R_3 + R_1 C_1 + R_2 C_2) + 1}}$$

Taking into account the actual fact that $C_2 \gg C_1$, by applying the Heaviside expansion formula, the current in the time domain is:

$$i(t) = (I_0 - I_1)e^{-\frac{t}{\tau_1}} + (I_1 - I_2)e^{-\frac{t}{\tau_2}} + I_2$$

where:

$$I_0 = \frac{E}{R_0 + R_{123}} \text{ - initial charging current}$$

$$I_1 = \frac{E}{R_0 + R_{23}} \text{ - final first-phase charging current}$$

$$I_2 = \frac{E}{R_0 + R_3} \text{ - final charging current}$$

$$\tau_1 = (R_0 + R_1)C_1 \text{ - time constant of the first phase}$$

$$\tau_2 = (R_0 + R_2)C_2 \text{ - time constant of the second phase}$$

In Figure 4 shows the current diagram according to the given expression.

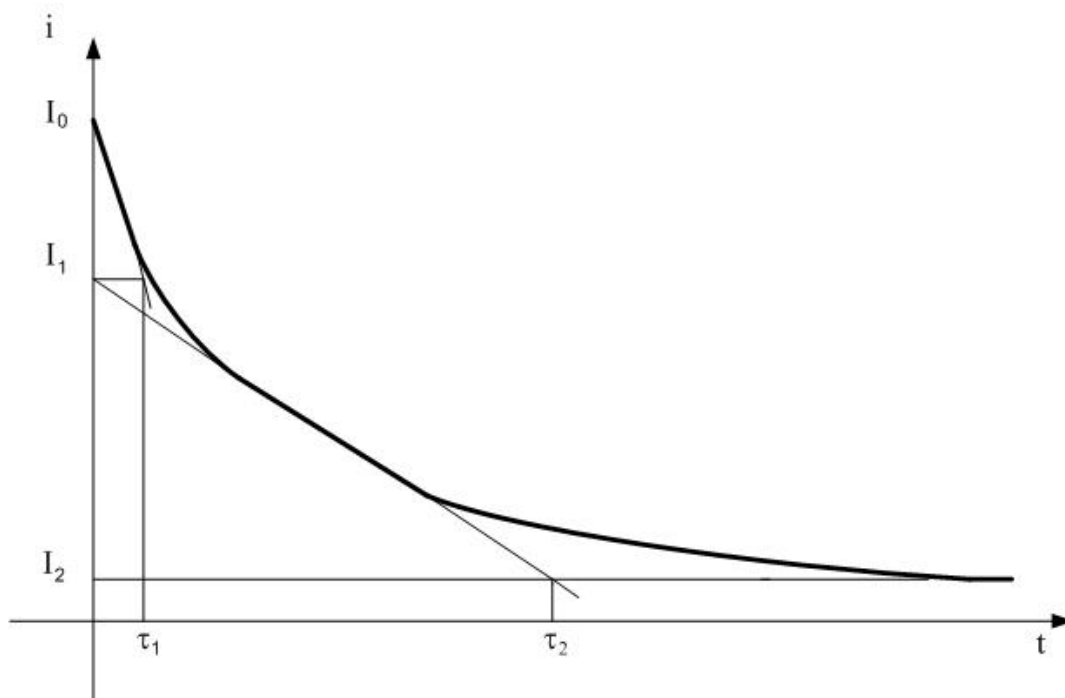


Figure 4. Potentiostatic excitation, current diagram

Based on the experimentally obtained current diagram, after reading the values $I_0, I_1, I_2, \tau_1, \tau_2$ the parameters of circuit can be determined:

$$R_3 = \frac{E}{I_2} - R_0$$

$$R_{23} = \frac{E}{I_1} - R_0$$

$$R_2 = \frac{R_{23}R_3}{R_3 - R_{23}}$$

$$R_{123} = \frac{E}{I_0} - R_0$$

$$R_1 = \frac{R_{123}R_{23}}{R_{23} - R_{123}}$$

$$C_1 = \frac{\tau_1}{R_0 + R_1}$$

$$C_2 = \frac{\tau_2}{R_0 + R_2}$$

This method has two major advantages over the other ones. Resistance R_3 can be the most reliably determined from the clearly discernible horizontal part of the curve, and also the time of the experiment is the shortest (lowest time constant of the second phase of charging).

2.3. Linear Sweep Voltage Excitation

System excitation is linear sweep voltage function as shown in Fig 5. The current in time as a response is monitored.

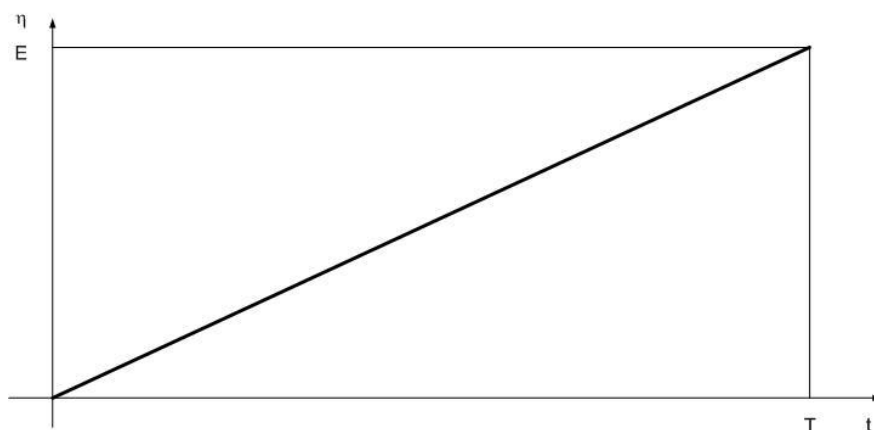


Figure 5. Linear sweep voltage function

As well as in the other methods, a second phase of charging is being considered, therefore equivalent circuit is simplified as shown in Fig 6.

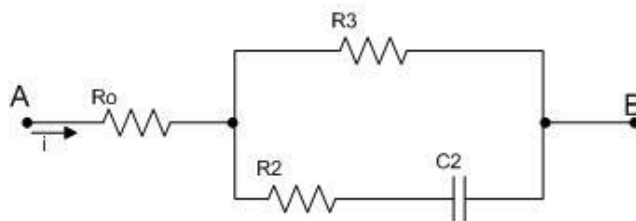


Figure 6. Equivalent circuit for second charging phase

The equation for the overvoltage in the time and frequency domain is:

$$\eta(t) = \frac{E}{T} \cdot t \cdot h(t)$$

$$\eta(S) = \frac{E}{S^2 T}$$

Impedance of the circuits is:

$$Z = R_0 + \frac{R_3 \left(R_2 + \frac{1}{SC_2} \right)}{R_3 + R_2 + \frac{1}{SC_2}} = \frac{S(R_0 R_2 + R_0 R_3 + R_2 R_3) C_2 + R_0 + R_3}{S(R_2 + R_3) C_2 + 1}$$

Complex image of current is:

$$I(S) = \frac{\eta(S)}{Z} = \frac{E}{T} \frac{SC_2(R_2 + R_3) + 1}{S^2(SC_2((R_2 + R_3)R_0 + R_2 R_3))} = \frac{E}{T} \frac{P(S)}{Q(S)}$$

Back in the time domain was carried out by the following procedure:

$$Q = 0 \Rightarrow S_1 = 0; S_2 = 0; S_3 = -\frac{R_0 + R_3}{C_2((R_2 + R_3)R_0 + R_2 R_3)}$$

Usually $R_0 \ll R_2 \ll R_3$, therefore:

$$Q_3 \approx -\frac{1}{(R_0 + R_2)C_2}$$

$$Q' = 2S(SC_2((R_2 + R_3 + R_2 R_3)R_0 + R_0 + R_3)) + S^2 C_2((R_2 + R_3)R_0 + R_2 R_3)$$

$$P(S_3) = -\frac{R_3}{R_2}$$

$$k_1 = \frac{1}{R_0 + R_3}$$

$$k_2 = \frac{(R_2 + R_3)R_3}{(R_0 + R_3)^2} C_2 \approx \frac{R_2 + R_3}{R_3}$$

$$i(t) = \frac{E}{T} \left(k_1 t \cdot e^{S_1 t} + k_2 e^{S_2 t} + \frac{P(S_3)}{Q'(S_3)} e^{S_3 t} \right) = \frac{E}{T} \left(\frac{1}{R_0 + R_3} t + C_2 \frac{R_2 + R_3}{R_3} - C_2 \frac{R_2 + R_3}{R_3} e^{-\frac{t}{\tau_2}} \right)$$

$$\tau_2 = (R_0 + R_2)C_2$$

Graphic current diagram is shown in Fig 7.

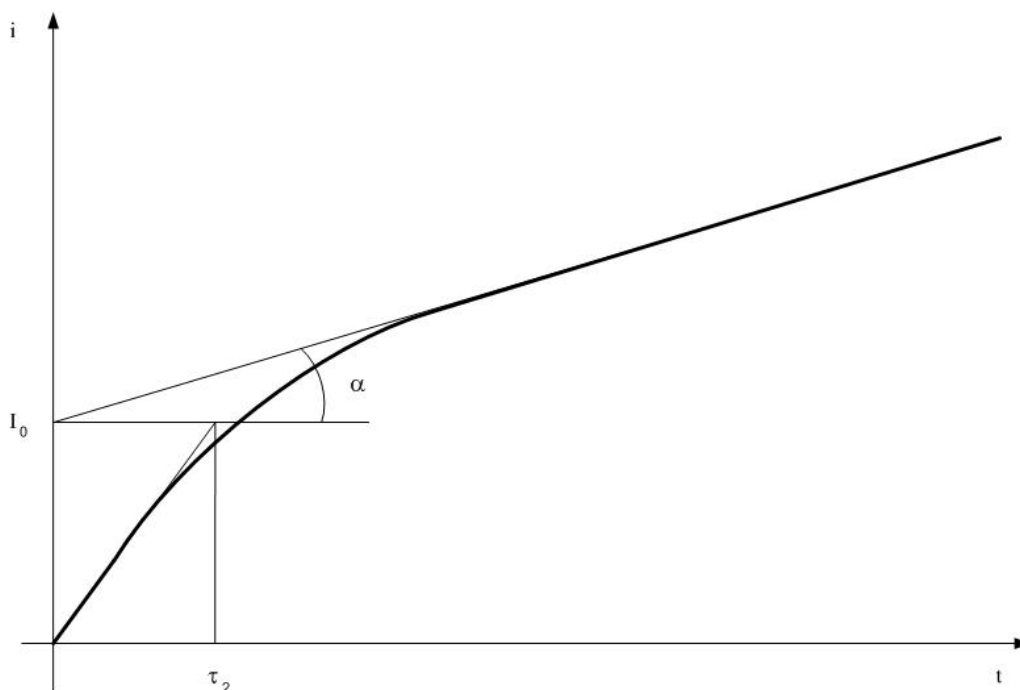


Figure 7. Current response diagram

Reading the values from the diagram, $tg\alpha$, I_0 and τ_2 (with the previously determined or estimated parameter R_0), parameter R_3 can be calculated:

$$R_3 = \frac{E}{T \cdot tg\alpha} - R_0; \quad tg\alpha = \frac{\Delta I}{\Delta t} \quad (\text{linear part of the curve})$$

From the system of equations:

$$I_0 = \frac{(R_2 + R_3)}{R_3} C_2$$

$$\tau_2 = (R_0 + R_2) C_2$$

R_2 and C_2 can be calculated.

In this way, the most important parameters of a supercapacitor have been determined, while at the same experiment is short term, and the destruction of the electrode is low.

2.4. Cyclic Voltammetry

Cyclic voltammetry is one of the standard methods in electrochemistry [25,26]. Excitation of the circuits is voltage signal as in Fig 8.

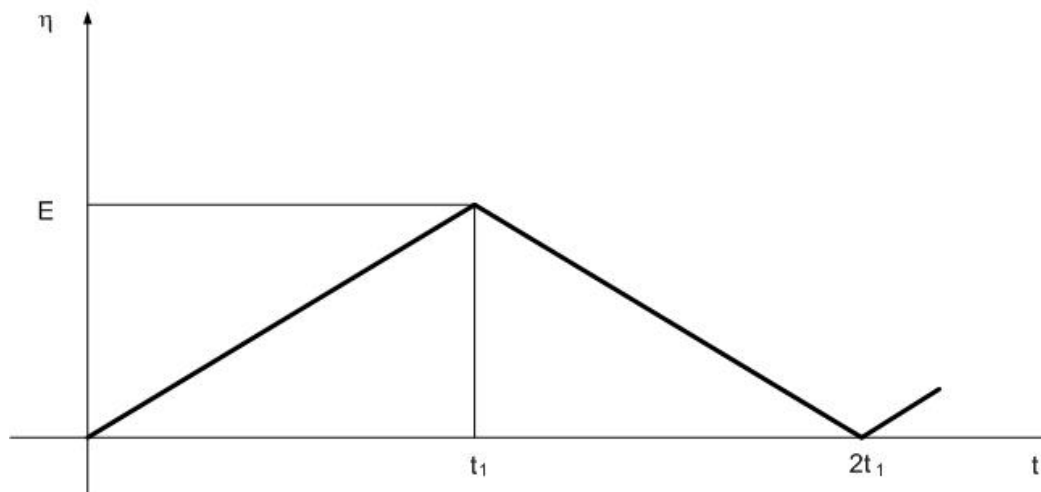


Figure 8. Excitation signal for cyclic voltammetry

As the response, input current in the time domain is monitored. Common name in electrochemistry is cyclic voltammetry, although the current is being measured, because the voltage at which current peak occurs is essential. In the case of supercapacitor, peaks are not expressed, because of the slow changes.

Excitation voltage can be expressed analytically as:

$$\eta(t) = \frac{E_m}{t_1} t \quad \text{for the arising area (charging phase)}$$

$$\eta(t) = 2E_m - \frac{E_m}{t_1} t \quad \text{for the falling area (discharge phase)}$$

With the realistic assumption that $R_0 \ll R_3$ and adding the condition $t_1 > 4\tau_2$ ($\tau_2 = R_2 C_2$ - time constant), by using the procedure similar to the linear sweep voltage function it leads to a simplified expressions for the current in the time domain in the quasi-stationary mode:

$$i(t) = \frac{E_m}{t_1} C_2 \left(1 - 2e^{-\frac{t}{\tau_2}} \right) + \frac{E_m}{2R_3} \quad \text{charge phase}$$

$$i(t) = \frac{E_m}{t_1} C_2 \left(2e^{-\frac{t}{\tau_2}} - 1 \right) + \frac{E_m}{2R_3} \quad \text{discharge phase}$$

The time is measured from the beginning of each stage. Obviously this is a complex form of current in time with exponential change of the AC component, and the DC component whose level is

$$I_{DC} = \frac{E_m}{2R_3}, \text{ therefore:}$$

$$I_{\max} = \frac{E_m}{2R_3} + \frac{E_m}{t_1} C_2 ; \quad I_{\min} = \frac{E_m}{2R_3} - \frac{E_m}{t_1} C_2$$

$$\frac{I_{\max} - I_{\min}}{2} = \frac{E_m}{t_1} C_2$$

Time diagram of the current is presented in the Fig. 9.

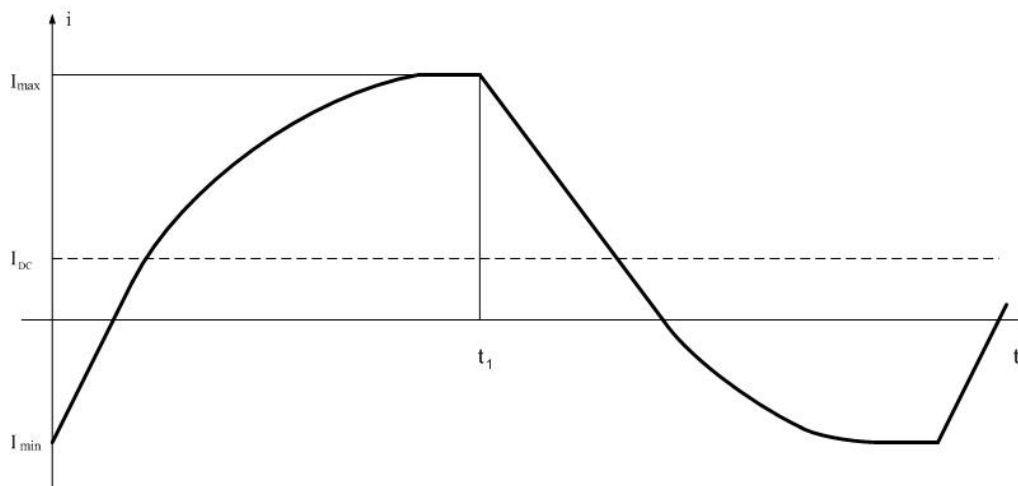


Figure 9. Responsive system current

Usually with this method, current is shown as the function of the excitation voltage, so the graph is obtained as shown in Fig 10.

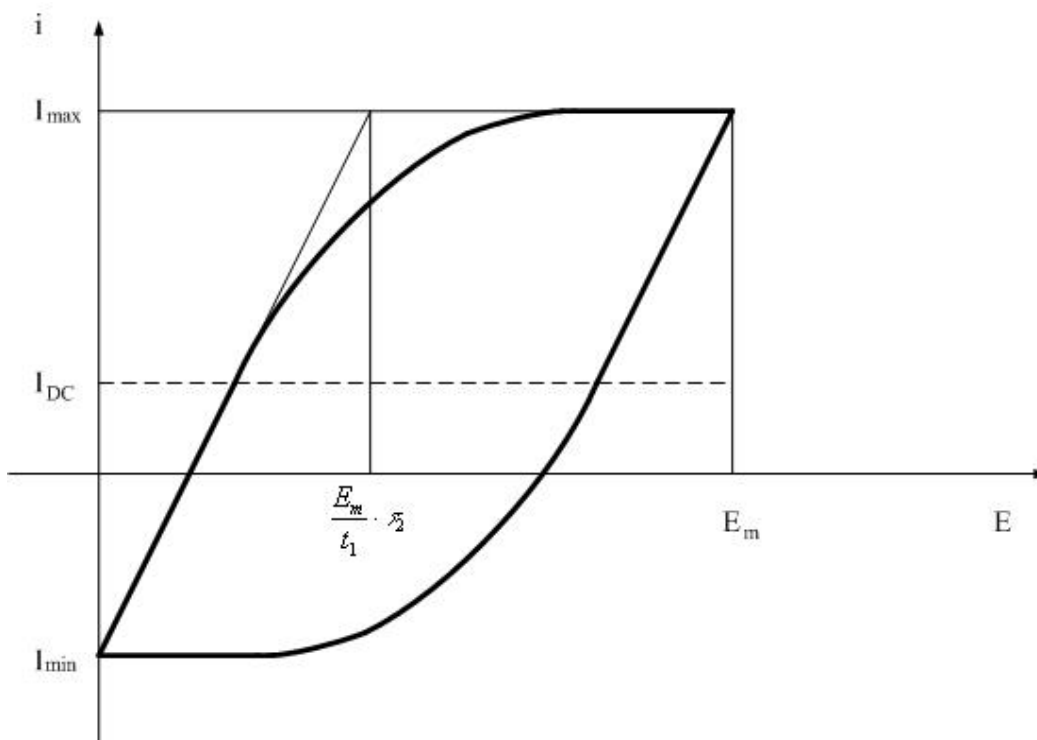


Figure 10. The cyclic voltammogram

Area of the shown loop (the electric power) is:

$$S_p = 2 \int_0^{E_m} i d\eta = 2 \int_0^{t_1} \frac{E_m}{t_1} C_2 \left(1 - 2 \cdot e^{-\frac{t}{\tau_2}} \right) \frac{E_m}{t_1} dt$$

$$S_p = 2 \frac{E_m^2}{t_1^2} C_2 (t_1 - 2\tau_2)$$

Based on these expressions, the procedure for the determination of the two most important supercapacitor parameters is:

1. From the recorded diagram as shown in Fig. 9, getting the values I_{max} and I_{min} so that the capacitance C_2 :

$$C_2 = \frac{I_{max} - I_{min}}{2E_m} t_1$$

2. From the same diagram, getting the time constant τ_2 , therefore the resistance R_2 can be calculated:

$$R_2 = \frac{\tau_2}{C_2}$$

It should be noted that C_2 can be determined from the expression for the loop surface that is more complex, but approximately applicable even if the experiment is not lead to the attainment of I_{max} , therefore it has shorter duration.

2.5. Linear Sweep Current Excitation

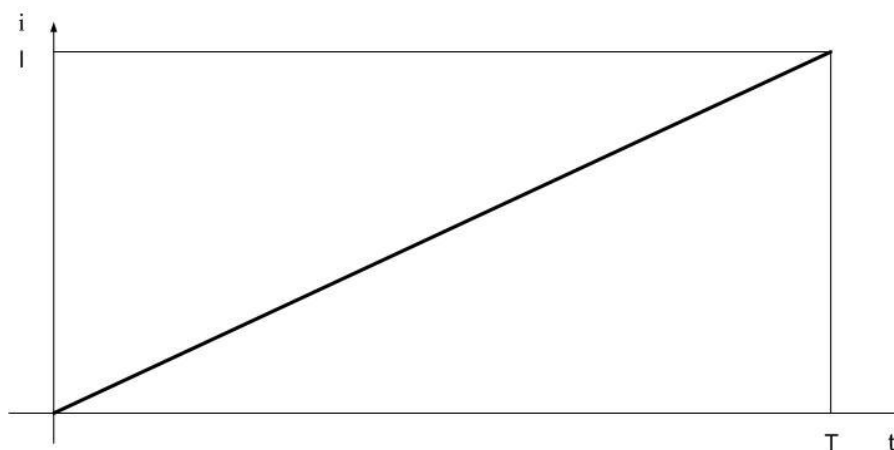


Figure 11. Diagram of linearly sweep current excitation

In this case, as the excitation it is applied linear current change over time (Fig 11.), and overvoltage η in charge was observed as a response. Depth analysis showed that this method clearly separates the first from the second charging phase (ie C_1 and C_2), so it is more suitable for reliable determination of the most important supercapacitor parameters, primarily C_2 . Therefore, in this section is presented the analysis of a second charging phase, or segment from which it is possible to determine important parameters of the supercapacitor.

Therefore, the analysis of the second charging phase, more precisely the segment from which the important supercapacitor parameters can be determined, is presented in this paper.

For the observed charging phase, system equivalent circuit is reduced to the one presented in Fig 11.

The expression for the current in the time and frequency domain is:

$$i = \frac{I}{T} t \cdot h(t) \qquad I(S) = \frac{I}{S^2 T}$$

Circuit impedance is the same as in linear sweep voltage excitation, so the complex image of overvoltage:

$$\eta(S) = U_{AB}(S) = I(S) \cdot Z = \frac{I}{T} \frac{SC_2(R_0R_2 + R_0R_3 + R_2R_3) + R_0 + R_3}{S^2(SC_2(R_2 + R_3) + 1)} = k \frac{P(S)}{Q(S)}$$

Since the polynomial Q (S) has a double root, the inverse Laplace transformation procedure is as follows.

$$Q = 0 \Rightarrow S_1 = 0; \quad S_2 = 0; \quad S_3 = -\frac{1}{C_2(R_2 + R_3)}$$

$$Q' = 2S(SC_2(R_2 + R_3) + 1) + S^2C_2(R_2 + R_3)$$

$$P(S_3) = \frac{R_3^2}{R_2 + R_3}$$

$$Q'(S_3) = \frac{1}{C_2(R_2 + R_3)}$$

$$K_1 = S^2 \frac{P(S_1)}{Q(S_1)} = R_0 + R_3$$

$$K_2 = \frac{d}{ds} \left[s^2 \frac{P(S_2)}{Q(S_2)} \right] = -R_3^2 C_2$$

$$\eta(t) = \frac{I}{T} \left(k_1 t e^{s_1 t} + k_2 e^{s_2 t} + \frac{P(S_3)}{Q'(S_3)} e^{s_3 t} \right)$$

$$\eta(t) = \frac{I}{T} \left((R_0 + R_3)t - R_3^2 C_2 + R_3^2 C_2 e^{-\frac{t}{\tau_2}} \right)$$

where $\tau_2 = (R_2 + R_3)C_2$ – time constant of the second phase of charging.

The expression for the overvoltage in the time domain is shown graphically in Fig 12. The equation of the asymptote for the presented graph is obtained from:

$$\eta(t)_{t \rightarrow \infty} = \frac{I}{T} \left((R_0 + R_3)t - R_3^2 C_2 \right)$$

Therefore, the intercept on the ordinate and the slope of the line are:

$$\eta_0 = -\frac{I}{T} R_3^2 C_2$$

$$k = \frac{I}{T} (R_0 + R_3)$$

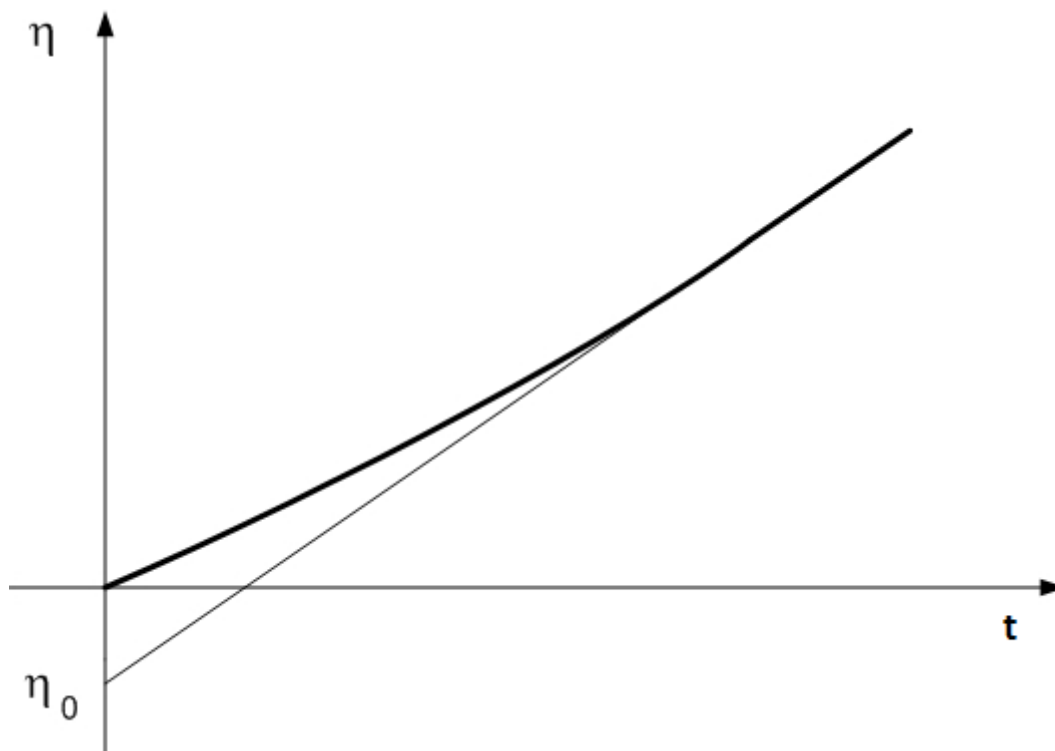


Figure 12. Diagram of the overvoltage

By getting η_0 and k from the diagram and including the values in the last two equations, the R_3 and C_2 can be determined, assuming that R_0 is determined by another method, or that it is negligible compared to R_3 .

3. RESULTS AND DISCUSSION

Electrochemical experiments have been performed in a standard three-electrode cell with saturated calomel reference electrode. Platinum electrode was used as a counter electrode [1,27-31]. Several working electrodes of different materials have been examined. This paper presents the results of the electrodes of chalcocite (Cu_2S , natural copper mineral).

Aqueous solutions of sulfuric acid, copper sulfate, sodium carbonate and sodium chloride p.a. purity have been used as electrolyte.

For each series of experiments, the working electrodes were honed, polished, washed and dried and then immersed in an electrolyte that was also fresh for the new series. Between the two experiments of the same series, polishing with rinse was performed. Grinding has been done with the finest sandpaper, polishing with alumina and rinsing with distilled water and alcohol.

All of the experiments were conducted at room temperature.

Physical model have been made according to the scheme in Figure 1, and it have been used for additional verification of the method. The values of the parameters: $R_0 = 3 \Omega$; $R_1 = 39 \Omega$; $R_2 = 90 \Omega$; $R_3 = 1\text{k}\Omega$; $C_0 = 0,12 \mu\text{F}$; $C_1 = 30 \text{ mF}$; $C_2 = 1,6 \text{ F}$.

3.1. Modified Galvanostatic Method

Galvanostatic experiments were performed according to previously described modified method for all of the working electrodes in various electrolytes. Starting from the adopted model, the parameters of equivalent electrical circuit for each system were determined and based on that further experiments were performed.

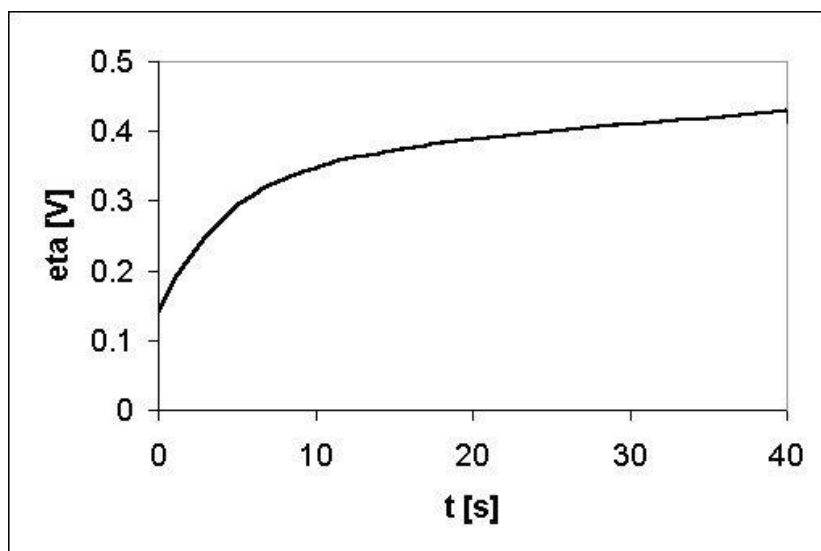


Figure 13. Physical model response on the galvanostatic excitation

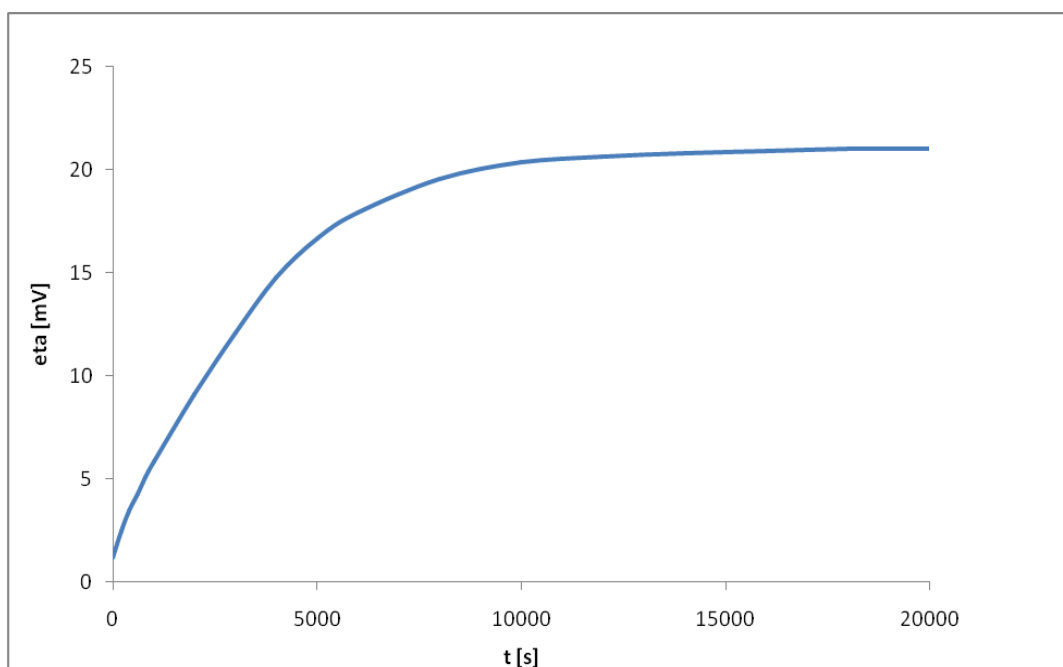


Figure 14. Galvanostatic curve for calcocite in a solution 1M H₂SO₄+0,1M CuSO₄ at excitation of 0,1 mA

Firstly, method and instrumental technique in the previously described physical model were checked once again. The intensity of the current pulse was 3 mA, and duration 40 s. The response of the circuit is shown in Fig. 13.

By getting characteristic values from the diagram and inserting those values into mathematical model, described previously in the analytical section, it is possible to define the parameters of the circuit:

$$R_1 = 38,6 \, \Omega; \quad R_2 = 91,5 \, \Omega; \quad C_1 = 29,2 \, \text{mF}; \quad C_2 = 1,56 \, \text{F}$$

which is in full compliance with the actual values. To determine the required R_3 , much longer experiment is needed, therefore this parameter is omitted.

Galvanostatic curve for chalcocite electrode (which was considered the most appropriate for) in a solution of sulfuric acid with the addition of copper sulfate at 0.1 mA excitation for a period of 20000 s is shown in Fig. 14. According to the diagram equivalent circuit parameters were calculated:

$$R_1 = 17,3 \, \Omega; \quad R_2 = 31,2 \, \Omega; \quad R_3 = 210 \, \Omega; \quad C_1 = 0,23 \, \text{F}; \quad C_2 = 33,1 \, \text{F}$$

The obtained values will be compared later with results obtained by other methods.

3.2. Potentiostatic Method

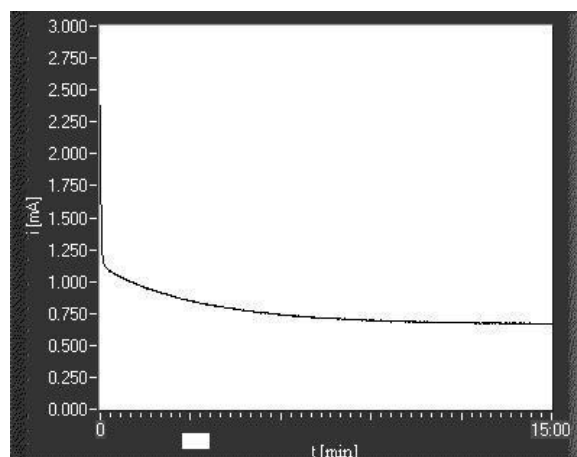


Figure 15. Potentiostatic curve for physical model at excitation of $\eta = 100 \, \text{mV}$

The method was firstly tested on a physical model with parameters: $R_0 = 3 \, \Omega$; $R_1 = 39 \, \Omega$; $R_2 = 90 \, \Omega$; $R_3 = 150 \, \Omega$; $C_0 = 0,12 \, \mu\text{F}$; $C_1 = 30 \, \text{mF}$; $C_2 = 1,6 \, \text{F}$. Excitation of $\eta = 100 \, \text{mV}$ with duration of 900s. Potentiostatic curve is presented in Fig.15.

By getting the characteristic parameters of the diagram (as described in the analytical section), the most important parameters of the circuit were defined:

$$R_2 = 91,1 \, \Omega; \quad R_3 = 148,8 \, \Omega; \quad C_2 = 1,63 \, \text{F} ,$$

which is in a full compliance with the actual parameters.

The advantage of potentiostatic methods - the relatively short duration of the experiment - was used to conduct further testing of the selected electrode (chalcocite) in various electrolytes, and in

order to select the optimal electrolyte in terms of obtaining the highest capacitance with minimal current leakage, therefore, the maximum value of R_3 .

Figure 16 shows potentiostatic curve (excitation at $\eta = 20$ mV) for chalcocite electrode in 1 M sulfuric acid together with 0.1 M copper sulfate.

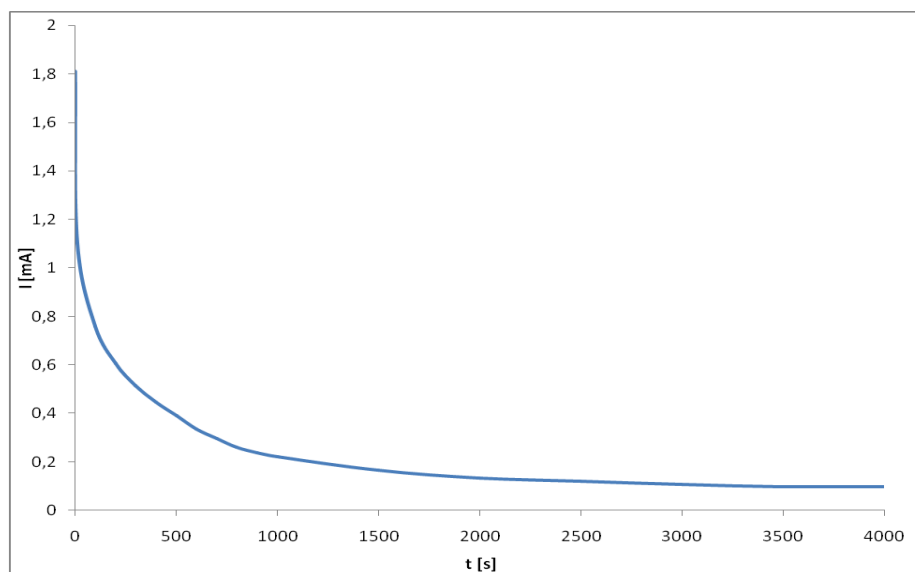


Figure 16. Potentiostatic curve for chalcocite electrode in solution of 1M H_2SO_4 +0,1M $CuSO_4$ at excitation of 20 mV

For such a optimized system, circuit parameters were obtained: $R_1 = 17,1 \Omega$; $R_2 = 30,8 \Omega$; $R_3 = 206 \Omega$; $C_1 = 0,22$ F; $C_2 = 31,8$ F.

3.3. Cyclic Voltammetry

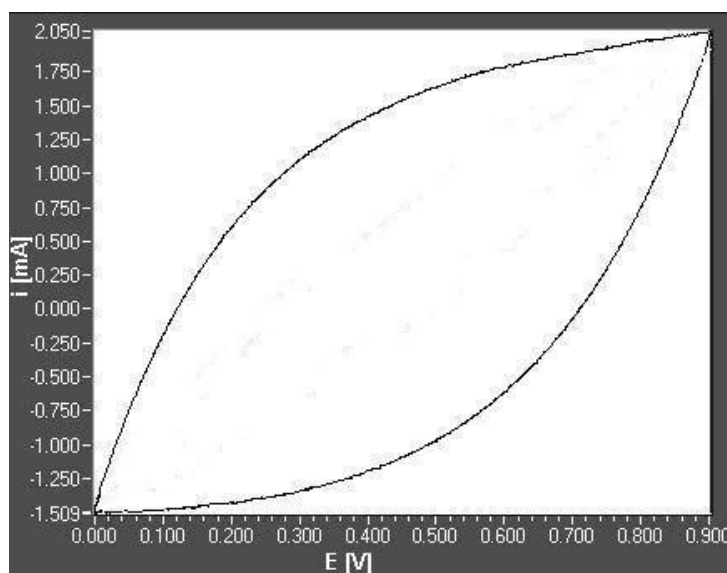


Figure 17. Physical model voltammogram at voltage increase speed of 1 mV/s

The classical method has been used with a very low speed voltage rise due to the high time constants of the investigated electrochemical systems.

The first measurements were conducted on a physical model with $R_0=3\ \Omega$; $R_1=39\ \Omega$; $R_2=90\ \Omega$; $R_3=1\ \text{k}\Omega$; $C_0=0,12\ \mu\text{F}$; $C_1=30\ \text{mF}$; $C_2=1,6\ \text{F}$ at a voltage increase speed of $dE/dt = 1\ \text{mV/s}$. Fig. 17 shows diagrams for $dE/dt = 1\ \text{mV/s}$. For the diagram obtained main parameters ($R_2 = 92\ \Omega$, $C_2 = 1,63\ \text{F}$) are in full compliance with actual data. Results show that it should apply as slow change of voltage as possible in order to obtain a wider loop, therefore, to reduce measurement errors.

Series of experiments with a variety of electrochemical systems and different voltage increase speeds were conducted in order to find optimal working conditions.

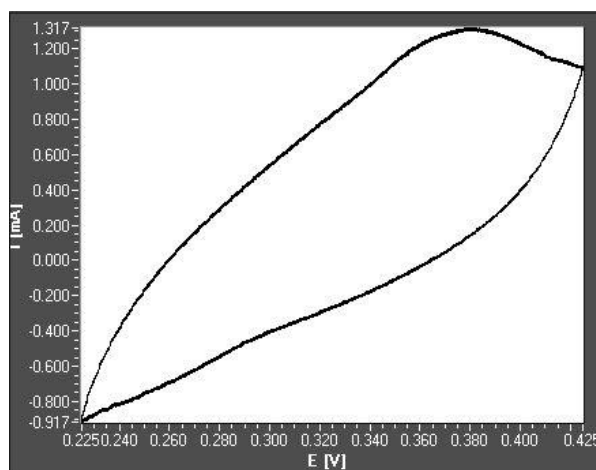


Figure 18. Voltammogram for H_2 in a solution of $1\text{M H}_2\text{SO}_4+0,1\text{M CuSO}_4$ at $dE/dt = 10\ \mu\text{V/s}$

Fig. 18 shows the voltammogram for the selected electrode (chalcocite) and the chosen electrolyte ($1\text{M H}_2\text{SO}_4+0,1\text{M CuSO}_4$) at voltage increase speed of $10\ \mu\text{V/s}$.

Surface of the loop was measured and from it the capacitance C_2 was determined: $C_2 = 32,2\ \text{F}$. Pulling the tangent to the initial part of the curve, time constant $\tau_2 = 1034\ \text{s}$ was determined, therefore $R_2 = \frac{\tau_2}{C_2} = 32,1\ \Omega$.

3.4. Linear Sweep Current Excitation

Due to the longer duration of the experiment, few typical systems were tested by this method. Fig. 19 shows response of an adopted electrochemical system (chalcocite in $1\text{M H}_2\text{SO}_4 + 0,1\text{M CuSO}_4$) at excitation $di/dt = 1,5\ \text{nA/s}$.

Based on the experimental curve, the parameters of the circuit have been calculated:

$$R_2 = 30,9\ \Omega; \quad R_3 = 201\ \Omega; \quad C_2 = 33,4\ \text{F}$$

which shows that the method can be used to easily determine important parameters of supercapacitor, but not all of them, so it must be combined with other methods.

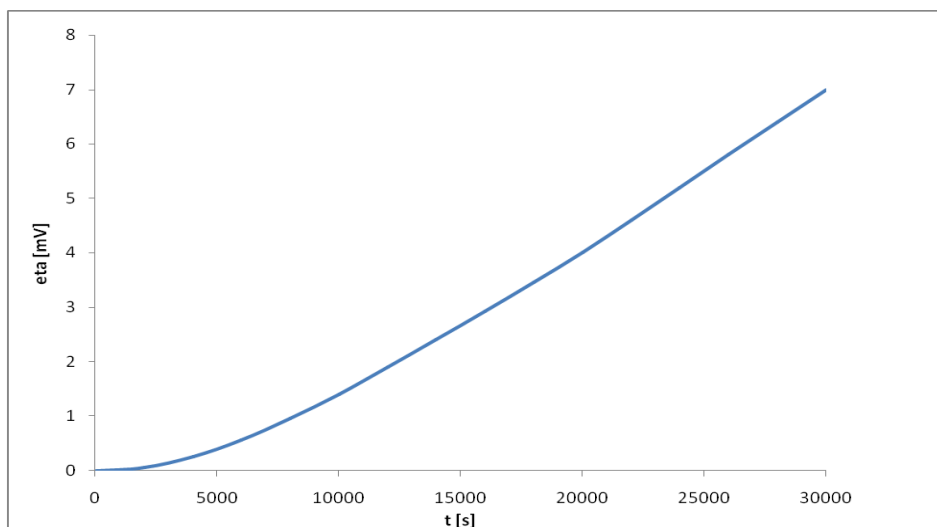


Figure 19. Response of the adopted system at tilting current excitation

3.5 Comparative Methods Review

In this section, a short review of the advantages and disadvantages of the methods will be presented, as well as tabular overview of the results.

In the case that the expensive equipment is not available or it is necessary to quickly determine the certain individual parameters, it is possible to use one of the fastest methods. The experiments show that the potentiostatic method provides satisfactory results with a shorter duration of the experiment, and even quicker, although rougher parameter determination, galvanostatic method can be applied. For a reliable determination of the capacitance C_2 , cyclic voltammetry can be applied, but with a long time experiment.

Table 1. below, shows the overview of the equivalent circuit parameters obtained by various methods for adopted electrochemical system.

Table 1. Overview of the measured parameters of the adopted electrochemical system

Method	R_1 [Ω]	R_2 [Ω]	R_3 [Ω]	C_1 [F]	C_2 [F]
Galvanostatic method	17,3	31,2	210	0,23	33,1
Potentiostatic method	17,1	30,8	206	0,22	31,8
Cyclic Voltammetry	-	32,1	-	-	32,2
Linear sweep current excitation	-	30,9	201	-	33,4

Since these are non-linear elements, and the methods are graphical, it can be concluded that the matching between the results is satisfactory. In addition to results matching of the methods described herein, well results matching has been found with the results obtained by other methods [32-34]. More accessible equipment has been used in here and developed mathematical models make it easier to conduct experiments.

4. CONCLUSION

Sulphide materials are poorly investigated from the standpoint of the electrode material for supercapacitors, therefore the presented researches are new to the area. The behavior of natural copper sulphide minerals, especially chalcocite (Cu_2S) in a solution of sulfuric acid with and without addition of CuSO_4 has been examined. Especially well behavior chalcocite has shown in solution $1\text{M H}_2\text{SO}_4 + 0,1\text{M CuSO}_4$. The results suggest the possible application of the shown system (memory and other electronic circuits with low power consumption), and also pave the directions of the further research in order to get even better parameters.

In order to do better investigation of the observed systems, the mathematical model is set, equivalent circuit was accepted and the comparative analysis was done for the standard electrochemical test methods (cyclic voltammetry and potentiostatic method), galvanostatic method is modified and new method is defined for this class of problems (linear sweep current excitation). Based on mathematical analysis all the parameters for experimental research are determined.

Series of the experiments has been conducted, both in the physical model and the real electrochemical systems. Based on obtained results, the model and test methods are verified, and also the electrochemical system is optimized. Also, the methods are compared in terms of efficiency and accuracy.

ACKNOWLEDGMENTS

The authors gratefully acknowledge financial support from the Ministry of Education and Science, Government of the Republic of Serbia through the Projects No. 172 060: “*New approach to designing materials for energy conversion and storage*” and Project No. 32043: “*Development and modeling of energy efficient, adaptive, multi-processor and multi sensor low power electronic systems*”.

References

1. B.E.Conway, Electrochemical supercapacitors, *Kluwer Academic/Plenum Publishers*, New York, (1999).
2. I.L. Skryabin, G. Evans, D. Frost, G. Vogelmann and J.M. Bell, *Electrochimica Acta*, 44 (1999) 3203-3209.
3. P.C.Butler, J.F. Cole, P.A. Taylor, *Journal of Power Sources*, 78 1-2 (1999) 176-181.
4. A.D. Pasquier, I. Plitz, J. Gural, S.Menocal and G. Amatucci, *Journal of Power Sources*, 113 1 (2003) 62-71.
5. Конденсаторы. Методы измерения электрических параметров. Общие положения. ГОСТ 21315.0-75, *Издательство стандартов*, 1976.
6. N.Khan, N. Mariun, M. Zaki and L. Dinesh, *TENCON 2000, Kuala Lumpur, Malaysia, Proceedings 3*, (2000) 193-199.

7. Y. Guo, J. Qi, Y. Jiang, S. Yang, Z. Wang and H. Xu, *Materials Chemistry and Physics*, 80, 3 (2003) 704-709.
8. G. P. Dai, M. Liu, D.M. Chen, P. X. Hou, Y. Tong and H. M. Cheng, *Electrochemical and Solid-State Letters*, 5, 4 (2002) E13-E15.
9. Z. Stevic, Ph.D thesis, *ETF Belgrade*, 2004.
10. C. Arbizzani, M. Mastragostino and L. Meneghello, *Electrochimica Acta*, 41, 1 (1996) 21-26.
11. M. Rajčić-Vujasinović, Z. Stanković and Z. Stević, *Elektrokhimiya*, 35, 3 (1999) 347-354.
12. C. Arbizzani, M. Mastragostino and F. Soavi, *Journal of Power Sources*, 100 (2001) 164-170.
13. Z. Stević, Z. Andjelković and D. Antić, *Sensors* 8, (2008) 1819-1831.
14. J.P. Zheng, J. Huang and T.R. Jow, *Journal of the Electrochemical Society*, 144, 6 (1997) 2026-2031.
15. J. Jamnik, J. Maier and S. Pejovnik, *Electrochimica Acta*, 44 (1999) 4139-4145.
16. W.C. West, K. Sieradzki, B. Kardynal and M.N. Kozicki, *Journal of the Electrochemical Society*, 145, 9 (1998) 2971-2974.
17. E. Barsoukov, J. H. Kim, K.S. Hwang, D. H. Kim, C.O. Yoon and H.Lee, *Synthetic metals*, 117, 1-3 (2001) 53-59.
18. P.J. Mahon, G. L. Paul, S. M. Keshishian and A. M. Vassallo, *Journal of Power Sources*, 91, (2000) 68-76.
19. Q. Yin, G.H. Kelsall, D.J. Vaughan and N.P. Brandon, *Journal of the Electrochemical Society*, 148, 3 (2001) A200-A208.
20. B. Pettinger and K. Doblhofer, *Can. J. Chem.* 75, 11 (1997) 1710-1720.
21. Ch. Lin, B. N. Popov and H.J. Ploehn, *Journal of the Electrochemical Society*, 149, 2 (2002) A167-A175.
22. H. Kim and B.N. Popov, *Journal of the electrochemical society*, 150, 9 (2003) A1153-A1160.
23. Hongqing Cao and Jingxian Yu, *Evolutionary Computation, CEC '03. The 2003 Congress on*, (2003).
24. R. Martin, J. J. Quintana, A. Ramos and I. de la Nuez, *Electrotechnical Conference, MELECON 2008, The 14th IEEE Mediterranean*, (2008).
25. W.G. Pell and B.E. Conway, *Journal of Electroanalytical Chemistry* 500, 1-2 (2001) 121-133.
26. M. Rajčić-Vujasinović, V. Trujić, Z. Stević and S. Đorđević, *3rd International Conference of the Chemical Societies of the South-Eastern European Countries on Chemistry in the New Millennium – an Endless Frontier, Book of Abstracts*, Volume I (2002) 337.
27. M. Antonijević and S. M. Milic, *Materials chemistry and physics*, vol. 118 No. 2-3 (2009) 385-391.
28. R. Markovic, J. Stevanovic, Lj. Avramovic, D. Nedeljkovic, B. Jugovic, Z. Branimir, J. Stajic-Trosic and M. Gvozdenovic, *Metallurgical and materials transactions b-process metallurgy and materials processing science*, vol. 43 No. 6 (2012) 1388-1392.
29. V.V. Panić, R.M. Stevanović, V.M. Jovanović and A.B. Dekanski, *Journal of Power Sources*, 195(13) (2010) 3969-3976.
30. V. Grekulovic, M. Rajcic-Vujasinovic, B. Pesic and Z. Stevic, *International journal of electrochemical science*, vol. 7 No. 6 (2012) 5231-5245.
31. H. Karami and A. Kaboli, *International Journal of Electrochemical Science*, 5(5) (2010) 706-719.
32. L. Borcea, Electrical impedance tomography, *Inverse Problems*, 18 (2002) R99-R136.
33. L. Kavan, P. Rapta and L. Dunsch, *Chemical Physics Letters*, 328 4-6 (2000) 363-368.
34. M. Itagaki, T. Ono and K. Watanabe, *Electrochimica Acta*, 44 (1999) 4365-4371.